

THE COMPUTER SIMULATION OF PROTON TRANSPORT IN BIOMOLECULAR SYSTEMS

Gregory A. Voth

Department of Chemistry and Henry Eyring Center for Theoretical Chemistry, 315 S. 1400 E., RM. 2020, University of Utah, Salt Lake City, UT, 84112, USA

TABLE OF CONTENTS

1. Abstract
2. Introduction
3. Molecular Dynamics Simulation Method
4. Applications
 - 4.1. Proton Transport in Bulk Water
 - 4.2. Proton Transport in Hydrophobic Channels
 - 4.3. Synthetic Leucine-Serine Channels
 - 4.4. Influenza A Virus M2 Channel
5. Concluding Remarks
6. Acknowledgements
7. References

1. ABSTRACT

A Molecular Dynamics computer simulation model for describing proton transport in biomolecular systems will be reviewed. The development of the underlying computational method which allows us to study the structural and dynamical properties of excess protons in these channels will first be discussed. Several applications of the methodology to study proton transport in channel environments will then be described. In each case, insight will be provided into the atomistic factors which determine the proton transport rate and the underlying mechanism(s) for the proton hopping process. More extensive background and results for the M2 channel in the influenza A virus will also be presented.

2. INTRODUCTION

The process of proton translocation is ubiquitous and extremely important in biology. For example, the energy that drives vital biological processes such as flagellar motion, active transport of ions, reduction of NAD^+ and NADP^+ , and ATP synthesis is stored within the electrochemical gradient; a gradient composed of a pH gradient (ΔpH) and a membrane potential ($\Delta \Psi$) (1). The force felt by the proton in this gradient is called the *proton motive force* (1, 2). ATP synthesis is catalyzed by the F_1F_0 -ATPase complex. The F_0 subunit of this complex is a channel imbedded in a membrane, be it the plasma membrane, the thylakoid membrane, or the inner mitochondrial membrane, and it serves as a reversible proton channel for the flow of protons down the membrane potential $\Delta \Psi$ (3, 4). Other important examples of proton transport are found both in bacteriorhodopsin and in the photosynthetic reaction center, where proton transport through water molecules and amino acid residues is a critical component of their overall function (5, 6).

For all of the above systems, and most certainly for the ones of interest to the Voth group (described in more detail below), it is a fascinating question whether nature simply *uses* water molecules in a directed manner to shuttle protons via Grotthuss hopping as they are needed for key biological functions (see Figure 1), or whether the ionizable amino acid residues of the biomolecular system must also directly participate in the proton translocation process (7).

A novel, accurate, and flexible Molecular Dynamics (MD) methodology will be reviewed below which is allowing our group to simulate the process of proton transport for the first time.

3. MOLECULAR DYNAMICS SIMULATION METHOD

In recent years our Voth group has developed an MD capability which allows for *explicit* proton transport within an *atomistic* and *deterministic* MD simulation context. The reader is referred to the published work on proton solvation and transport in bulk water, weak acids, hydrophobic channels, the water/lipid bilayer interface, and most importantly, through large transmembrane proton channels such as the M2 channel in influenza A and the synthetic LS2 channel (8-18)

The atomistic MD simulation approach relies on our Multi-State Empirical Valence Bond (MS-EVB) model to describe the proton shuttling process (see the left panel of Figure 2) (9, 10, 14). In this approach, the various possible protonation configurations of the water molecules are modeled by limiting "states", which in turn compose the basis states in an overall Hamiltonian matrix. There are also

Computer Simulation of Proton Transport

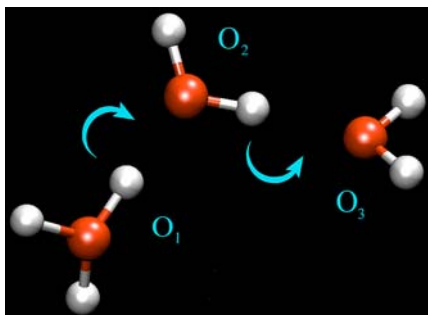


Figure 1. The Grotthuss proton shuttling process in water.

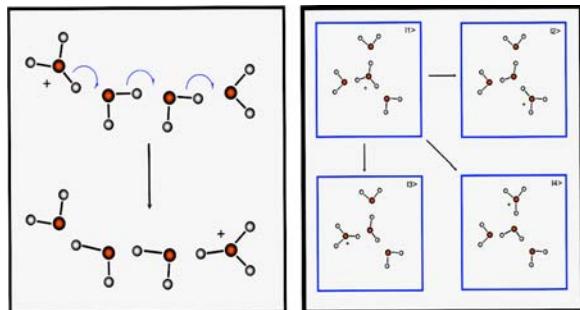


Figure 2. Left panel. The Grotthuss process. Right panel. The four MS-EVB states necessary to model the Eigen cation H_9O_4^+ in the gas phase. In the condensed phase, more than 30 states are required to model the excess proton and its solvation shells.

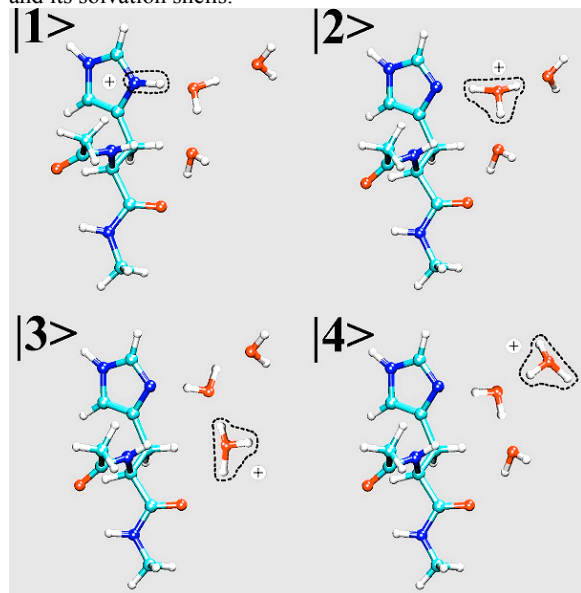


Figure 3. The first four MS-EVB states required to model histidine protonation/deprotonation in water.

off-diagonal elements in this matrix that allow for transitions to occur between the various states as a function of the instantaneous nuclear configurations, and hence the chemical and hydrogen bonding topology varies along with it as a function of time. In the right-hand panel of Figure 2, the four MS-EVB states necessary to model the gas phase H_9O_4^+ Eigen cation are shown as an example to help illustrate the concept. It should be noted that in the bulk

phase, however, many more states are necessary (as many as 40 in order to describe the first three solvation shells of a hydronium ion in bulk water). Each state contains *all* of the molecules of the condensed phase system, but with the excess proton bonded to a different molecule in each state. Then, for any given nuclear configuration and time step in the MD simulation, the MS-EVB Hamiltonian matrix is diagonalized and the lowest state eigenfunction determined. The forces on the nuclei are next calculated using the Hellmann-Feynman theorem for this state and fed into an MD integrator such as Velocity Verlet. The procedure is iterated and an MD trajectory is generated which *includes explicit proton shuttling through water molecules*. Such MD trajectories, when properly averaged, have been shown to reproduce the experimental bulk water proton mobility, spectroscopic data, and the deuterium isotope effect in bulk water (10-12, 14, 19).

Importantly, the MS-EVB method was developed to be compatible with, and transferable to, molecular mechanics (MM) force fields such as AMBER. In fact, the MS-EVB methodology is fully implemented within a Voth Group version of the DL_POLY MD code (and already applied, for example, to study proton transport near biological membranes and a large viral proton channel, as described later). The basic MS-EVB algorithm is *parallelized* in this code, so the computational overhead associated with the EVB state structure is efficiently distributed over processors. (Note that the vast majority of the pair-wise interactions in a realistic application of the MS-EVB approach do not contain the excess proton complex and hence involve no more computational expense than a classical biomolecular MD simulation.) Furthermore, a systematic approach has been developed to define the parameters of both the diagonal and off-diagonal MS-EVB matrix elements in order to accurately reproduce various high level *ab initio* results for binding energies and proton transfer barriers, as well as bulk phase proton structural, transport, and spectroscopic properties.

There is also an ongoing effort in the to increase the accuracy and generality of the underlying fundamental MS-EVB methodology. For example, the approach is being extended to include the effects of electronic polarizability and general acid-base ionization, all on the same dynamical footing as the proton transport. The MS-EVB model has also been recently extended to treat multiple excess protons and hence constant pH conditions (Tharrington, *and collaborators*, to be published). This advance in the MS-EVB simulation methodology will allow for a comparison with the experimental conductance versus pH curves in channels such as gramicidin A, especially in the cases for which multiple proton occupancy may be important.

The extension of the MS-EVB method to include weak acids has proven to be extremely important because it allows for *explicit dynamical protonation and deprotonation of ionizable amino acid residues* in channels and enzymes, such as the histidine group shown schematically in Figure 3 (this extension is important for the simulations of M2 channel described later). In essence, the fundamental deprotonation step (involving states “1”

Computer Simulation of Proton Transport

and “2”) is in turn embedded within the bulk water MS-EVB state structure (for which two states, “3” and “4”, out of many possible involved in the subsequent proton shuttling, are shown). This approach allows seamless integration of these processes into the overall MS-EVB MD algorithm, and the final model reproduces both *ab initio* (binding energy, geometry, barriers) and experimental (e.g., pK_a in pure aqueous solution) results.

Some comments are also in order on how the MS-EVB MD simulation methodology relates to that of others. It must be appreciated that the original EVB method was developed by Warshel and co-workers in order to study proton and hydride transfer in enzymes, as well as electron transfer reactions (20). Generally these applications required a two-state EVB parameterization. The MS-EVB approach represents a non-trivial generalization of these ideas to describe proton *transport* over much longer distances, involving shuttling through many water molecules and possible ionizable groups. It should further be noted that Vuilleumier and Borgis, evidently taking a lead from the original 2-state EVB work for the excess proton in water, independently developed their own multi-state model for bulk water (21-23). However, there are important differences between their approach and MS-EVB, particularly in the treatment of the off-diagonal matrix elements, the state selection algorithms, and the energy conservation properties. It should also be noted that the latest generation MS-EVB model (MS-EVB2) and its underlying algorithm has taken a significant departure from some of the initial concepts (14).

In principle, one might also be able to relate the effective EVB states in the MS-EVB model to more explicit electronic states although the more empirical route has proven to be quite successful (25). Other simulation approaches for proton transport have also appeared in the literature (26, 27). However, most of these do not have the multi-state character of the MS-EVB approach and hence do not allow for the important process of proton charge delocalization over multiple water molecules. Yet another model has also appeared in which proton transport is treated as a stochastic hopping process of the proton overlaid on an MD trajectory (28). As computationally efficient as such a non-deterministic approach may be, it does not seem clear how it tells one anything decisive about the underlying molecular interactions responsible for the proton transport mechanism in biomolecular systems, nor how the parameters of such a model can be developed in an independent fashion. One interesting technique has recently been developed that has been successful in modeling proton *transfer* reactions between well-defined donor and acceptor groups in, e.g., enzymes (29). However, the ability of this approach to study proton transport for long time scales (multi-ns), over long distances (10 to 40 Angstroms) and through intervening solvent water molecules and amino acid residues, is not clear given its large computational cost with increasing system size.

Within any MD simulation methodology it is also important to consider exactly what one will calculate. Often MD simulations are used, with good effect, to study

structural issues in proteins. In terms of kinetics, MD can also be invaluable in calculating *free energy* barriers within a transition state theory context (if done correctly) and, if one is fortunate, the trajectories utilized in these calculations may reveal important information about the underlying atomistic interactions that influence the free energy barrier. Proton transport over long length and time scales is rather different in that it can involve numerous free energy barriers and subtle dynamical effects such as long time scale protein conformational changes. In some cases such as the M2 channel described below, the first (and perhaps most important) question is a binary one, i.e., is the channel open or is it closed? (It will be described how this well-defined question will be addressed in the next section, based largely on structural arguments.) In other systems such as the synthetic LS2 and LS3 proton channels (or the M2 channel when it is in an open state), one can seek a deeper analysis, which might involve calculating the potential of mean force (PMF) through the channel of the excess protonic charge (which can be characterized by the center-of-excess-charge, or CEC, coordinate, which will be described in the next paragraph). The PMF, in essence, provides a picture of the free energy landscape sampled by an ensemble of excess protons as they diffuse through the channel. More explicitly, one could then model this process by a diffusion or Poisson-Nernst-Planck (PNP) equation with the PMF providing the barriers to free diffusion. (The calculation of an accurate PMF, over the full length of a channel such as the M2 or LS2 channel, is no small feat, requiring both novel and extensive sampling techniques.) Ideally, for any biomolecular system, one should also calculate the actual (dynamical) diffusive behavior of the excess proton, because it is not clear how well phenomenological approaches such as Eyring theory or the PNP equation fit reality. This is especially true for proton transport through water and ionizable amino acids inside proteins, since transient proton “wires” can be formed for which proton hopping dynamics are anything but diffusive for the brief lifetime of the proton wire. As will be described later for the M2 channel, these transient wires can be coupled to protein fluctuations, so the picture is quite complex, requiring an analysis of individual trajectories beyond just the calculation of a PMF to move the excess proton from point A to point B. If, on the other hand, subtle dynamical events have any statistical significance in the larger picture, their effect should somehow be seen in the PMF because the proton is, after all, moving from one region to another within the protein.

A few comments are in order here on the calculation of the PMF for proton translocation. An important quantity in this regard is the “center-of-excess-charge” (CEC) coordinate, which could be readily defined in the MS-EVB model as a way to characterize the “location” of the excess protonic charge. This is not such an easy thing to do because the Grothuss shuttling involves many protons, so there is no single “excess proton”. In the MS-EVB model, however, the CEC can be defined as the expectation value of the charge over the EVB state space, hence leading to a clear definition of the excess charge location, similar in many ways to a center-of-mass variable. This definition is proving to be invaluable in the MS-EVB

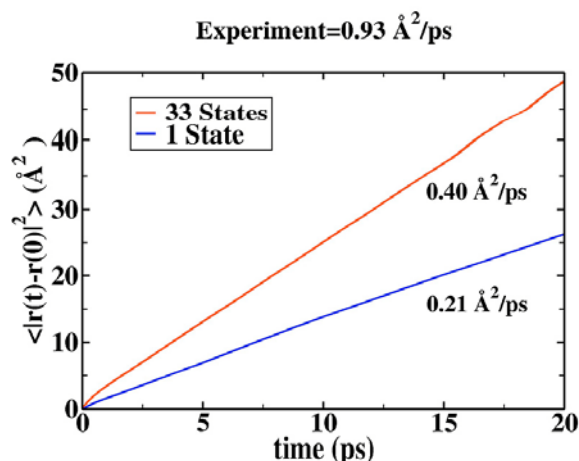


Figure 4. The mean-squared displacement of the excess proton center-of-excess-charge in bulk water. The 33-state result is for the full MS-EVB simulation, while the 1-state result is for the classical diffusion of the hydronium with no Grotthuss shuttling allowed.

MD simulations of proton translocation in the biomolecular context, i.e., the PMF of the CEC can be calculated along a generalized reaction coordinate such as the the z-coordinate of the CEC for a trans-membrane channel aligned along the z-axis, or the spherical distance of the CEC from a donor or acceptor site of an enzyme. The free energy barriers of the PMF are often found to be more than several kcal/mol high, thus inhibiting a direct sampling along the whole reaction path during a normal MD run. Sampling is readily enhanced, however, by adding an extra “umbrella” potential to the system Hamiltonian in terms of the CEC coordinate. As long as the umbrella potential is a function of the reaction coordinate(s) only, the unbiased probability distribution is related directly to the measured distribution in the extended system. If different parts of the phase space are sampled by separate umbrella simulations, the overall PMF can be reconstructed by the Weighted Histogram Analysis Method (WHAM), which has become standard practice (30).

In MS-EVB MD simulations of proton transport in realistic biomolecular systems, we generally hope to adopt the following procedure: (1) First, one must ask and answer qualitative questions such as identifying the conformations of the protein at hand that allow proton transport to occur in the first place (e.g., the open and closed states of M2). (2) One should next calculate the PMF for proton transport process in order to reveal its barriers and bottlenecks. In some cases, one may add constraints to the motion of key residues and/or calculate two-dimensional PMF’s to better understand a larger free energy picture involving these groups. Finally, (3) one can and should perform extensive analysis of many individual trajectories to help reveal the origins of certain key features of the PMF and to look for important and interesting dynamical effects such as concerted (coherent) proton transport motion and important conformational fluctuations of the surrounding protein. This computational methodology is underway for the M2 and LS2/LS3 proton channels.

With the MS-EVB MD approach in hand, a rigorous and ambitious research effort to study proton transport in key biomolecular systems is now underway. Several applications, including bulk water, a hydrophobic channel, the synthetic LS2 and LS3 channels, and the influenza A M2 channel, will now be described.

4. APPLICATIONS

4.1. Proton Transport in Bulk Water

In order to be able to accurately simulate proton transport in biomolecular systems, one must first be able to reliably simulate the proton transport process in bulk water. For this reason, significant effort was first invested to finish the development and validation of the basic MS-EVB model for the excess proton in liquid water (9, 10). It was shown that the model could reproduce the self-diffusion properties for the hydrated proton, as well as its solvation structure, infrared spectroscopy and observed deuterium isotope effects (10, 12, 14, 19). A second-generation (MS-EVB2) model was also developed that incorporates simpler electrostatics and improved energy conservation characteristics via a more advanced EVB state selection algorithm (14). An MS-EVB approach for treating weak acids and ionizable amino acid residues was further developed (see Ref. 8, Cuma *and collaborators*, 2001; Soudackov and Voth, to be published).

Shown in Figure 4 is the mean-squared displacement of the excess protonic charge as a function of time in bulk water. The red line is for the full MS-EVB2 model, in which 33 MS-EVB states are required to describe the bulk phase proton solvation and Grotthuss shuttling process. The blue line is for the 1-state limit of the MS-EVB2 model, in which all proton shuttling has been artificially “turned off” so that only normal, hydrodynamic diffusion of the hydronium ion can occur. This result is quite interesting because it shows that the Grotthuss shuttling only contributes about a factor of two to the proton transport rate in bulk water, suggesting that this factor could be significantly enhanced in a more confined biomolecular environment. Importantly, the diffusion constant from the classical MS-EVB MD simulation is below the experimental result by about another factor of two, which is to be expected because the above simulations involved *classical* nuclei. Path integral Centroid Molecular Dynamics (CMD) simulations for the MS-EVB model in fact showed that the quantum effects on the proton transport rate are about a factor of two consistent with the observed deuterium isotope effect of around 1.6 (12, 31-33).

A few comments are also in order regarding the efforts of others to simulate the excess proton in aqueous environments. Perhaps the most notable of these efforts are those of Parrinello and co-workers using the Car-Parrinello method for *ab initio* MD (34, 35). In this approach, the electronic structure at the level of gradient-corrected density functional theory is solved simultaneously with the nuclear dynamics. This innovative method can reduce the uncertainties associated with empirical force fields, but it comes at an enormous computational cost. In the case of

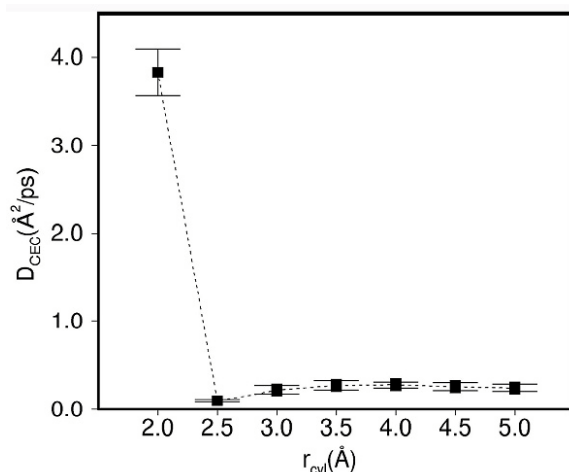


Figure 5. The diffusion constant of the excess proton in an idealized hydrophobic channel as a function of channel radius. The 2.0 Angstrom channel allows only a 1-dimensional “water wire” to exist in its interior.

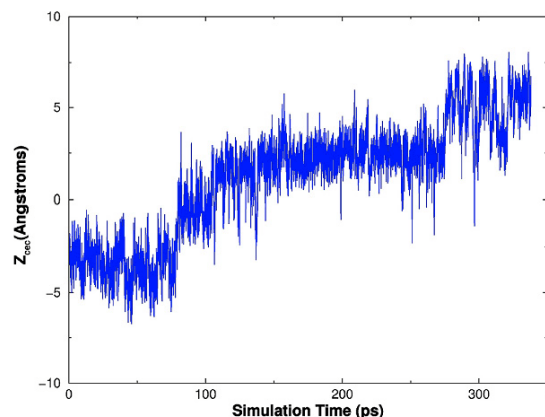


Figure 6. A trajectory of an excess proton inside the gramicidin A channel.

the excess proton in bulk water, important information could be obtained on its solvation structure and a few Grotthuss hopping events could be observed. However, these simulations are severely limited in their duration (generally ten or less ps) and in their size (usually no more than about 64 water molecules, periodically replicated). By contrast, the MS-EVB simulations necessary to accurately calculate the bulk diffusion rate of the hydrated proton required an averaging over numerous (ten or more) very long (ns) trajectories, each of which exhibited 100 or more Grotthuss hopping events. The scale of the simulations needed to adequately simulate proton translocation in biomolecular environments is even greater still. Another approach to proton translocation has been taken by Pomès and Roux in which they have studied proton translocation in water wires and simplified models of the gramicidin A system using the PM6 model for dissociable water (36-40). This latter approach may be questioned given that the PM6 model does not yield accurate results for the excess proton in water and it gives anomalously low barriers to proton transfer in protonated water clusters.

With the MS-EVB model development in hand, the focus next turned to the biomolecular context as will be described in the following subsections. It should be noted, however, that the evolution of the fundamental MS-EVB approach continues in a complementary and synergistic fashion. This includes the development of an electronically polarizable MS-EVB model, an autoionizable MS-EVB model for water, and various simulation studies of proton solvation and transport in water clusters, water-alcohol mixtures, and at the water-vapor interface.

4.2. Proton Transport in Hydrophobic Channels

One of the first applications of our MS-EVB model was to study the transport of protons through narrow hydrophobic channels filled with water (15). In some ways, this modelistic study defines the *theoretical limit* of proton transport behavior through water in confined channel geometries. This work, in fact, revealed a dramatic enhancement of the proton transport rate when a hydrophobic channel is so narrow that only a single file chain of water can be supported (i.e., a “water wire”). Plotted in Figure 5 is the diffusion constant of the excess proton as a function of hydrophobic channel radius, with the narrowest channel giving a large enhancement of about a factor of 20 in the diffusion constant over that of the wider channels. (The latter channels having values similar to the bulk water proton diffusion value.) This result, which was the first of its kind using a *realistic* interaction model for protons shuttling through water molecules, suggests that stable water wires in narrow hydrophobic channel domains such as in cytochrome c oxidase can indeed yield significant proton translocation rates. Interestingly, at the same time this work was published, Hummer and co-workers discovered that water could spontaneously fill solvated narrow carbon nanotubes in realistic MD simulations, thus proving our study to not be so modelistic after all (41). Subsequently, the MS-EVB MD approach has been used, along with *ab initio* MD, to study proton transport through these water-filled tubes, and a proton transport rate of a factor of 40 greater than that in bulk water was observed—a value very close to that which was predicted from the model hydrophobic channel two years earlier (42).

By contrast, a very different MS-EVB MD result shown in Figure 6 is the proton hopping dynamics in the single file water wire of the *gramicidin A* (gA) channel (the latter being embedded in a hydrated DMPC lipid bilayer). Depicted is a single trajectory of the CEC which describes the location of the excess protonic charge in the gA channel water wire. This trajectory, which is similar to numerous others we have found for gA, reveals quite different dynamics than the rapid CEC diffusion seen in the ideal narrow hydrophobic channel. Instead, one sees long periods of relative stability in the channel (little diffusion along the channel axis) interrupted *infrequently* by *significant hopping events*. These hopping events are seen in Figure 6 around 75 and 275 ps in the trajectory, and they last for only 5-10 ps in duration. The individual trajectory result shown here *suggests that it is the transient formation of the water wires involving the excess proton and at least three water molecules that defines the rate of proton*

Computer Simulation of Proton Transport

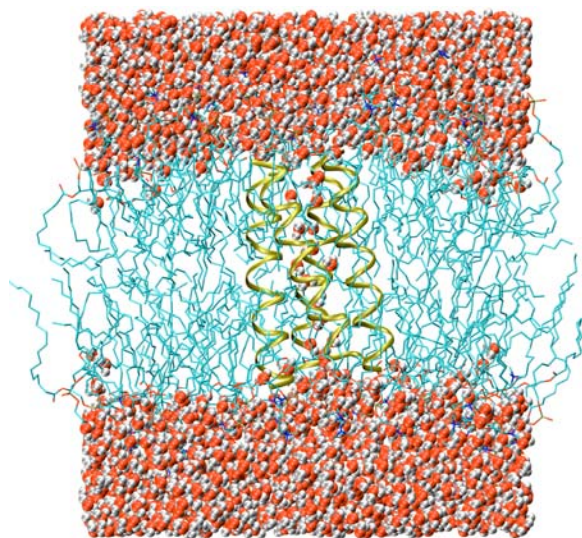


Figure 7. The synthetic LS2 proton channel in POPC bilayer.

translocation through the gA channel. The relatively long periods of stability of the CEC in gA reflect the *hydrophilic* nature of the channel, i.e., the microsolvation of the excess proton and the overall water wire by the channel residues (especially carbonyl groups). The above dynamical result is also in contrast to the concept of the “turning defect” of water dipoles in the channel as providing the origin of the free energy barrier to proton translocation (39). In the simulations based on the more accurate MS-EVB model, the individual water dipoles in the channel distant from the protonic charge, *while it is in the channel*, already seem to rotate considerably due to their thermal motion, so it seems unrealistic to envision a collective dipole turning process in the channel (i.e., the “turning defect”) being distinct from the process of proton translocation through the channel. From these results, it can be anticipated that proton transport in most realistic biomolecular hydrophilic domains may occur via shuttling through *transient water wires*, which live only for short durations in time. This also suggests it is critical to have a simulation methodology such as MS-EVB in which the proton and its hopping through the transient water wires is *treated explicitly*.

4.3. Synthetic Leucine-Serine Channels

Natural channels often have complex structures that may make the analysis of proton transport processes through the pore difficult. Synthetic ion channels having a minimalist design can avoid some unimportant, but complicating, factors while still preserving the essential features of a channel. The leucine-serine (LS) system is an example of such a minimalist approach. This system includes two ion channels, having the amino acid sequences as follows: Ac-(LSLLLSL)₃-CONH₂ (LS2) and Ac-(LSSLLSL)₃-CONH₂ (LS3). Experiments have shown these two channels can form ion channels in a lipid bilayer that can conduct protons in a voltage-gated manner (43-46). Despite its similarity in amino acid sequence, the LS3 channel exhibits much larger ion conductance than the LS2. While, the LS3 channel also displays greater proton conductance than the LS2 channel under experimental

conditions (900 pS vs. 120 pS), it can readily conduct other monovalent cations, such as Li⁺, Na⁺, K⁺, Cs⁺, and Guanidinium⁺, unlike the LS2 (44). The molecular origins of these important differences are largely unknown and very interesting.

Based on the assumption that the LS channels have symmetric oligomeric structures in the active state, it has been suggested that the LS2 channel tends to form a parallel homo-tetramer structure while the LS3 channel favors a hexamer (44). The oligomeric structures are actually bundles of the amphiphilic α -helices, in which the serine side chains form the hydrophilic face while the leucine side chains form the hydrophobic face. This kind of α -helix bundle is a typical ion channel architecture. The reason the LS3 helix favors a hexamer is thought to be related to the fact that its hydrophilic face is larger, making it more stable to surround a wider water column (46).

The LS ion channels have also been the subject of several simulations), including from the present project (47-51). The dynamics of the helices, overall channel stability, and pore waters have been the main targets of analysis. The detailed process of proton transport inside these channels remains poorly understood and, until now, could not be explicitly simulated by MD methods. Research on the explicit proton transport in these channels will be highly valuable in understanding their important similarities and differences. Moreover, while synthetic channels such as the LS system are not found in nature, their relative simplicity is useful in answering many fundamental questions about proton transport in channels. Perspectives concerning water dipole orientation in the pore, reorganization energy of intra-pore water, and lipid/protein interaction effects on proton transport are all important topics of which our understanding is minimal, at best. In addition, these peptides have been synthesized and studied in the laboratory, so they are not purely computer models as are many channels in idealized computational studies.

Preliminary classical MD simulations of the two leucine-serine synthetic proton channels embedded in a fully-solvated lipid bilayer revealed a significant difference in the dynamics of the pore water molecules (50). While both channels were in a presumed open state in the simulations, the pore water in the narrower channel (LS2) exhibited a much lower diffusion constant. This finding may account at least in part for the much smaller proton conductance and proton selectivity of the LS2 channel. However, MD simulations of explicit proton solvation and transport in these channels are essential, so in this spirit the first such MS-EVB study was carried out recently for LS2 (51). In the first part of these studies, a fully equilibrated LS2 system was obtained in POPC bilayer, including full Ewald treatment of the long range electrostatics (see Figure 7). Because it was desired to run many, very long MS-EVB simulations to study the proton solvation behavior in the channel, the subsequent simulations were performed on a reduced LS2 channel system, in which only the protein and the water molecules near or inside the channel were included. The channel structure was further stabilized by

Computer Simulation of Proton Transport

relatively loose position restraints on the backbone atoms. This system reduces the computational expense while preserving many essential features of the channel, such as its geometry and the diffusion constants of the pore water. Analysis of the solvation states of the excess proton in different channel regions along the z -axis discovered a non-uniform association of the proton as a function of the local channel pore size. In the wider channel regions (roughly 2.1 Å in radius), the excess proton tended to adopt the Eigen solvation structure (H_9O_4^+), while in the narrow channel regions (roughly 1.6 Å in radius), the stability of the Zundel solvation structure (H_5O_2^+) with respect to the Eigen structure was increased (or even surpassed that of the Eigen in some cases). The same trend was also observed in the MS-EVB simulations of the excess proton in idealized hydrophobic channel environments discussed earlier (15).

The LS2 MS-EVB study also revealed that the proton solvation structure in this channel is very sensitive to its local micro-environment. For example, even in the channel regions with similar pore radii, the excess proton exhibits quite different solvation structures. In particular, in three of the five wider channel regions, the excess proton was found to display high preference for the Eigen solvation structure, which suggests these regions may behave like barriers preventing the excess proton from more efficient transport via the Grotthuss mechanism. It was also found that removing the partial charges of the serine side chains has a dramatic effect on the excess proton's solvation structure, which suggests the intimate involvement of the channel walls in the solvation of the excess proton. Structural analysis further showed that the Zundel solvation structure can be stabilized by forming hydrogen bonds between the pore water and the serine side chains symmetrically on both the proton donor and acceptor sides. Within a larger picture concerning proton transport in biological systems, these LS2 results may imply that the excess proton's solvation inside a hydrophilic protein environment can be tightly-controlled by the side chain conformational dynamics, through complicated interactions among the excess proton, the channel water molecules, and the channel side chains. This perspective is certainly consistent with our results on the more complicated M2 system (discussed below), illustrating both the importance of the synthetic channel studies and the need for more extensive simulations of these systems in the future.

4.4. Influenza A Virus M2 Channel

The influenza A virus M2 channel is a proton selective channel that has been found to play essential roles in the viral life cycle. During the viral uncoating process, when the virion is internalized into the endosome, the M2 protein can acidify the virion interior, promoting the dissociation of the viral matrix protein (M1) from the ribonucleoprotein (RNP), which is a crucial step for the transport of the RNP from the virion into the cell's nucleus (52-56). For some influenza virus subtypes, it has been found that the M2 channel can elevate the intravesicular pH of the trans-Golgi network, preventing a viral protein haemagglutinin (HA), which is transported to the cell surface through the trans-Golgi network, from incorrect

maturation in an otherwise low pH environment (57-60). Blocking the M2 channel by the anti-flu drug amantadine (1-aminoadamantine hydrochloride, AMT) has been shown to interrupt both parts of the viral life cycle (58, 59, 61, 89) critical roles of the M2 channel in the viral life cycle, study of its structure and function at various levels of molecular detail is of great interest to anti-flu drug design, pharmacology and medicine.

The 19-residue trans-membrane (TM) domain of the M2 protein is the main channel-forming structure which is directly responsible for multiple molecular functions: the selective filter, the channel gate, and the interaction sites of the AMT inhibitor. This domain can form one α -helix strand that is able to span the hydrocarbon region of the membrane (63, 64). A considerable amount of experimental evidence has indicated that the structure of the M2 channel is a parallel homotetramer in the TM domain (54, 63-69).

A synthetic 25-residue peptide (M2-TMP) with the amino acid sequence corresponding to residues 22-46 (encompassing the segment for the TM domain, residues 25-43) of the M2 protein has been found to form an AMT-sensitive proton-selective channel in lipid bilayers with similar specificity and efficiency to the full M2 protein (68, 70). It has been shown to form tetramers in lipid micelles (66, 68). Spectroscopy experiments have determined the helix tilt angle with respect to the membrane normal (30–40°) and the rotational angle around the helix axis (roughly -50°) (71-75). These tilt angles suggest that the M2-TMP channel should be left-handed so that the hydrophilic residues can be oriented towards the pore lumen (71). Recently, the tilt angle for the TM domain of the full M2 protein in liposomes was also determined, revealing a smaller value of $25^\circ \pm 3$ (69). The reduced tilt angle could be due to stronger inter-subunit interactions in the whole protein.

The M2 channel is highly proton-selective — at least 10^6 -fold more proton conductive than for other cations, and it is low-pH gated, undergoing a 50-fold conductance increase from pH 8.2 to pH 4.5 (76-78). Strong evidence has suggested that His37, which is highly conserved in all strains of influenza virus and is the only ionizable residue in the TM domain (around pH 6), plays a crucial role (78-80). Several recent experimental studies have also suggested the involvement of the Trp41 residue in channel gating (81-83). Though the actual structure responsible for these functions remains unclear, two possible proton conductance mechanisms, namely the gating mechanism and the shuttle mechanism, have been proposed.

In the postulated gating mechanism, one or more of the histidine imidazole moieties can be protonated and become positively charged when the channel is activated (see Ref. 84, Sansom *and collaborators*, 1997). The protons are not immediately released back to the pore water; instead, the histidine residues bind them (for a relatively long time). Then, due to the electrostatic repulsion between the positive charges, the imidazole side chains swing away from each other, thus opening the

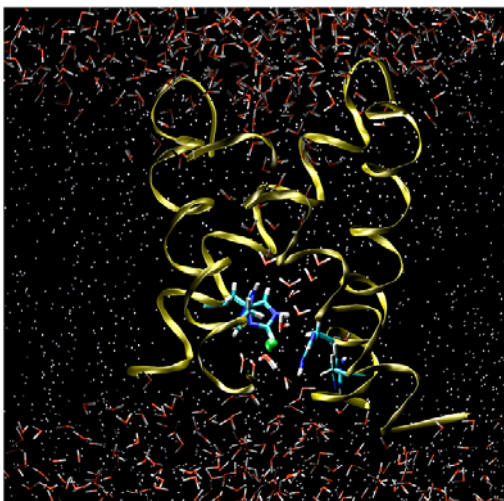


Figure 8. The M2 transmembrane proton channel from the influenza A virus. The green ball is the excess proton moving through a transient water wire in the gating region, as shown from an MS-EVB MD simulation of the channel.

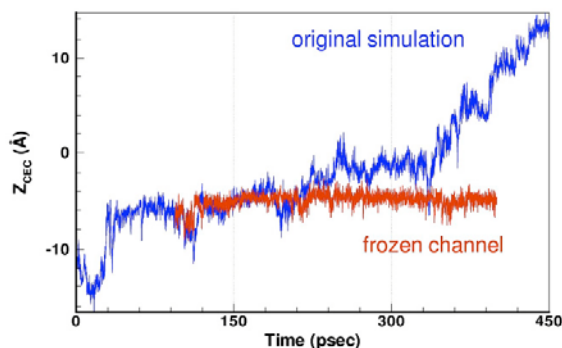


Figure 9. Two trajectories of the excess proton location in the axial direction of the M2 channel versus time. The frozen channel has constraints on the M2 helices, and the proton transport is seen to shut down in this case, reflecting the importance of the channel fluctuations.

otherwise occluded pore to let the pore water penetrate through, forming a continuous proton-conductive water wire. In the next section, our MD results will be described which have shown a mechanism similar to this conductance mechanism explicitly in operation for the first time.

In contrast to the gating mechanism, the histidine residues in the proposed shuttle mechanism are proposed to be directly involved in a proton relay (63). In this mechanism, when the channel is activated, an imidazole side chain accepts the excess proton to form a bi-protonated intermediate, which is presumed to be short-lived and tends to release either the ϵ - or δ -hydrogen back to the pore water to become neutral again (proton shuttling). Transport of a single proton through the gate is accomplished when the hydrogen at the opposite side is released to the pore water. Then to transport the next proton, the initial state needs to be regenerated, which is hypothesized to occur through tautomerization or a simple flipping of the imidazole ring.

Perhaps the most important result obtained to date using the MS-EVB method is the MD simulation of explicit

proton translocation through the M2 channel (17). The simulation was carried out on the TM domain of M2 in a fully-solvated DMPC bilayer with the assumption that one stable bi-protonated His37 might lead to the opening of the channel for protons. Seven MD simulation trajectories were obtained with different starting configurations, in all of which the excess proton was placed inside the channel at different positions near the extracellular N-terminus of the M2 channel. Indeed, within the time scales reached by the simulations (1 ns for each trajectory), the proton was observed to pass through the channel in three of the seven trajectories. In addition, a temporary opening of the pore at the constrictive region formed by the His37 residues was observed when the excess proton approached this region. These results lend direct support to a variant of the gating mechanism; however, as opposed to the picture of the gating mechanism described previously, our MD study suggests that one (or maybe two) bi-protonated histidines may be sufficient for opening the channel for protons while still keeping it closed for other ions. Moreover, the presence of one positive charge near the constrictive region formed by the His37 residues seems to not lead to a barrier too high for protons to pass through.

A snapshot taken from one of the MS-EVB MD simulation trajectories of the M2 proton channel is shown in Figure 8. The channel backbone helices are shown as coiled tubes, while the side chains of the His37 residues, which form the constrictive gate region, are shown in stick mode. The excess proton is represented as a green ball, near which the pore water molecules are shown as sticks. The two water molecules directly involved in the first solvation shell of the excess proton are highlighted with thicker sticks. Note the transient single file water wire formed in the gate region that the excess proton shuttles through. A movie of one of these MS-EVB proton transport trajectories may be viewed at the URL www.hec.utah.edu/~gazz/nmovie.mov. (Note that the orientation of the channel is inverted in this movie so the intracellular side is at the top.)

The MS-EVB MD study of the M2 channel also provides critical information on the factors affecting the explicit proton transport in the channel for the first time. For example, it was confirmed that, as in bulk water, the excess proton in the channel is actually shuttled via the *structural diffusion* mechanism, where the excess proton's solvation structure rather than the hydronium ion is propagated in space (13, 34). It was also found that the excess proton favors an Eigen-like solvation structure in the channel similar to that in bulk water; however, its overall diffusion constant is reduced in the channel by up to a factor of three, or it may even be immobilized in some situations for long periods of time. Importantly, the MS-EVB simulations also illustrate the important influence of the channel *dynamics* on proton's motion in the channel. By placing artificial constraints on the channel helices, the proton transport through the channel was seen to be completely "turned off." This behavior can be seen from a comparison of the two CEC trajectories in Figure 9. Plotted is the progress of the CEC through the channel as a function of time. The blue trajectory is for the fully

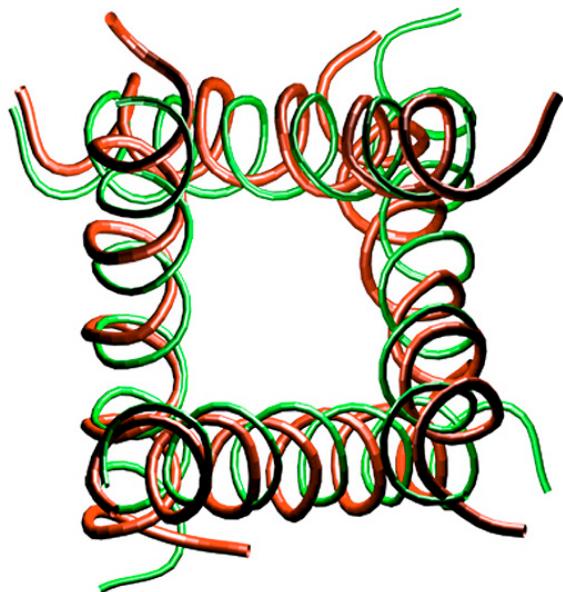


Figure 10. The M2 channel viewed from above. The red helices are from the MD simulation while the green are inferred from NMR experiments.

unconstrained case, while the red trajectory is for the case when the channel helices are constrained. Clearly, the dynamical fluctuations of the helices in the lipid bilayer environment have a significant qualitative effect on the proton transport dynamics. This finding is especially interesting because it confirms that proton transport through water regions in proteins can depend on the *dynamical environment of the entire protein*, not just the structure and dynamics of the water through which the proton is shuttling. The MD results also again confirm that transient water wire configurations are critical for the proton transport process. In this case, a brief 50 ps or so of the blue (unconstrained) trajectory, beginning around $t = 370$ ps, represents the onset of proton transport through the His37 bottleneck region via a proton wire.

The proton conductance mechanism will continue to be a goal of future MS-EVB MD studies of the influenza A M2 channel. One goal must be to calculate a converged PMF for the proton transport through the channel. A considerable amount of experimental evidence has also suggested that the highly conserved residue His37 plays a crucial role in the channel's selectivity and the channel gate (78-80, 84). As previously mentioned earlier, in one proposed mechanism for proton conductance in the channel the His37 residue is directly involved in the proton relay system (the shuttle mechanism) (63). In another proposed mechanism, protonation of this residue structurally transforms the channel from a closed to an open state (the gating mechanism), as was seen in our MD study of explicit proton transport in the channel (17, 84).

Clearly, however, not all of the important aspects of the proton transport process were addressed in our first MS-EVB study of M2. For example, a non-ionizable histidine model was used with the assumption that a singly-

protonated His37 residue is stable and does not release a proton to solvent for at least the time scale the simulation (nanoseconds). This assumption can will be explored in the future and explicitly removed with the development of our ionizable histidine MS-EVB model as described in Sec. B (Soudackov and Voth, to be published). Furthermore, the current MS-EVB MD simulation capability will enable more than one excess proton to be simulated in the system, which means the proton conductance mechanism can be analyzed in terms of multiple protons in the channel, thus facilitating the study of the relationship between proton transport of the de/protonation of the His37 residue in greater detail. One can also explore the following features of the system: (i) The pK_a and the free energy of de/protonation of the His37 residue can be calculated from the MS-EVB MD simulations. An experimental value for the pK_a is known (68) and can be used to validate these results; (ii) The dynamics of this amino acid upon de/protonation as well as its influence on the other residues can be characterized, which will provide a more detailed view of the molecular motions when the channel's open/close state changes; (iii) The effects of mutations of amino acids will be explored, such as the H37G mutation (Pinto, unpublished) (iv). The effects of all of these features can be related to the behavior of the PMF of an excess proton transporting through the channel.

We have also compared the M2 channel model used in our MD simulation work with an NMR backbone structure of the M2-TMP channel determined by Cross and coworkers (75). The average tilt angles for each helix in our MD simulations are 47° , 42° , 39° , 38° with standard errors around 10° , placing them in good agreement with the experimental value of 38° . The averaged rotational angles for each helix are 12° , 1° , -22° , -20° , deviating somewhat from the reported experimental value ($-62^\circ - -43^\circ$). However, our model is perhaps the best example achieved yet for the M2 system using computer modeling without using any previous knowledge of experimental structural data. A superimposed picture of the averaged backbone structure from the simulation (red) on the NMR structure (green) is shown in Figure 10. Some comparisons between other computer models and the NMR structure may be found in the literature, and generally these exhibit significantly worse agreement (75). We are currently refining the underlying MD model using the most recent OPLS force field and the preliminary results are very encouraging regarding the rotational angles. It should also be noted that there are important differences between the experimental conditions and the lipid bilayer environment in our MD simulations (86).

One of the most critical issues for the M2 channel research is to identify the actual closed state of the channel and to observe it remaining closed even in the presence of explicit excess protons in the MS-EVB MD simulations. Along these lines, several recent experimental studies have suggested the involvement of the Trp41 residues in channel gating. For example, a UVRR spectroscopy study has suggested that Trp41 may have cation- π interaction with the bi-protonated histidine residue in the open state (82). Through mutagenesis and electrophysiological

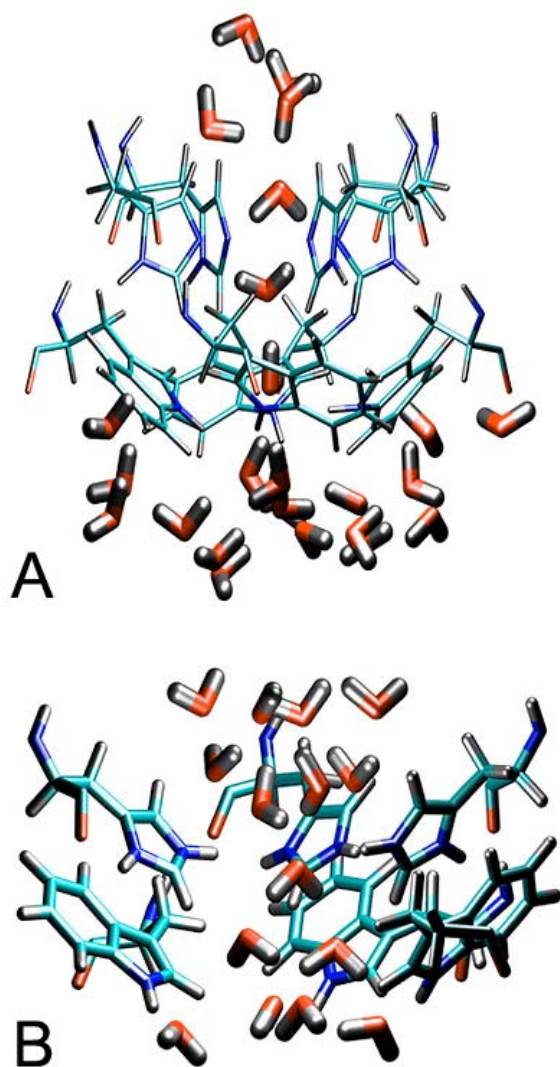


Figure 11. Possible closed (left panel) and open (right panel) states of the M2 channel identified from a search of the rotamer library and electronic structure calculations. Note the hydrogen bonding structure in the closed state which would presumably prohibit proton shuttling.

experiments, Pinto and coworkers have proposed the Trp41 residue may be the actual channel gate (83). Cross and coworkers have recently determined that the distance between the N_{δ} -His37 and C_{\square} -Trp41 should be less than 3.9 Å for the closed channel further implying the involvement of Trp41 in channel gate. Based on this information and the previously determined NMR backbone structure, the (t-160, t-105) conformation was proposed by them for His37 and Trp41. [The notation – (t-160, t-105) – means that the conformations of His37 and Trp41 are the t-160 and t-105 rotamers, respectively (81). The nomenclature for rotamers here follows the Penultimate Rotamer Library (87). When the mono-protonation state of the histidine is taken into account, the symbol δ or ϵ is added – for example, (t-160, t-105, δ) – to indicate the histidine is δ - or ϵ -mono-protonated, respectively].

The conformation of these residues is tightly coupled with the proton transport mechanism, and we have recently carried out preliminary investigations on this issue. Based on the same experimental structural information, our preliminary computational results support an alternative conformation – (t60, t90, δ) – for the closed state of the M2 channel (81). This result was obtained by cross-checking energetically-favorable conformations (from *ab initio* calculations) with those found to agree functionally with experiment. The conformations for which these analyses were performed were determined using a thorough scan over the conformational space. A representative structure of this conformation is seen in the left panel (a) in Figure 11 and shows that a constrictive region is formed by *both* His37 and Trp41. This model seems consistent with almost all of the experimentally observed phenomena regarding His37 and Trp41. For example, the pore waters have an *opposing hydrogen-bonding orientation* near His37, explaining why the channel does not conduct protons in this closed state if the histidine residues are neutral. The conformation of Trp41 prevents His37 from being exposed to the bulk water at the C-end, suggesting why protons cannot be transported outward. The four ϵ -nitrogen atoms from His37 can form a Cu^{2+} chelating site, explaining the inhibition of the channel by Cu^{2+} . Interestingly enough, the opposing orientation of the water molecules near His37 is similar to the orientation found in an MD simulation of aquaporin a channel that conducts water but is impermeable to protons. It is fascinating that this hydrogen bonding motif, apparently designed by Nature to block proton transport through a channel such as aquaporin, seems to have appeared again in the M2 channel (88).

The orientation of His37 in the above proposed closed structure is also not consistent with the shuttle mechanism proposed by others. It was therefore necessary to find an open structure into which the closed structure can evolve upon protonation. This structure was found by a rotation of the histidine's χ_2 angle from 60° to 0° , which leads to a pore wide enough to let water penetrate through it (see panel (b) of Figure 11). The close contact between His37 and Trp41 in this open structure favors a cation- π interaction between these two residues. An MD simulation with this open structure was also performed in which *all* histidine residues were in a bi-protonated state in order to examine a previously proposed gating mechanism (82, 85). It was found that the fully bi-protonated state leads to a highly ordered pore water structure whose orientation would likely preclude proton transport from the N-terminus to the histidine residues.

Combining these preliminary results and our previous MS-EVB simulation results, an alternative gating mechanism can be suggested as follows: The closed structure has the (t60, t90, δ) conformation. When the pH_{out} goes down, one (or maybe two) histidine residue becomes bi-protonated, at which point it undergoes a small conformational change by rotating its χ_2 angle from 60° to 0° so that it can be stabilized by its nearest tryptophan residue via a cation- π interaction. This change and other conformational adjustments triggered by it opens the pore to let pore water penetrate, forming a proton-conductive

Computer Simulation of Proton Transport

water wire through the gate region as we have witnessed in our MS-EVB MD simulations (17). Protons can then diffuse through channel by hopping through the pore water molecules via the Grotthuss shuttle mechanism. Clearly, one important target for our future research will be to explicitly verify our proposed gating mechanism through MS-EVB MD simulations in both the open and closed states, including the calculation of the PMF for both states and analysis of explicit proton transport trajectories, as well as dynamical protonation/deprotonation of one or more of the His37 residues. The influence of mutations studies on our proposed gating mechanism will also be explored.

5. CONCLUDING REMARKS

In this paper, a unique and ongoing MD simulation methodology has been outlined which allows for the study of explicit proton translocation in a variety of biomolecular contexts. Key results have been summarized for bulk water, a model hydrophobic channel, synthetic leucine-serine proton channels, and the M2 proton channel in the influenza A virus. In all cases, important insights have been revealed on the underlying structural and dynamical features which affect the proton transport process in these interesting systems. It is anticipated that many new and more comprehensive studies of proton translocation in biomolecular systems will be undertaken in the future.

6. ACKNOWLEDGEMENTS

This research was supported by the National Institutes of Health (GM-53148) and the National Science Foundation (CHE-9712884). I wish to acknowledge the many students and postdoctoral fellows who have contributed to this research, including Alexander Smondyrev, Udo Schmitt, Yujie Wu, Alexander Soudakov, Tyler Day, Arnold Tharrington, Stephanie Atherton, Martin Cuma, Mark Brewer, Harald Tepper, Matt Petersen, Gary Ayton, Srinivasan Iyengar, and Christian Burnham. This work would not have been possible without their extraordinary efforts and creativity.

7. REFERENCES

1. Stryer, L.: Chapter 39: Excitable membranes and sensory systems; Chapter 13: Metabolism: Basic concepts and design; Chapter 17: Oxidative phosphorylation. In biochemistry eds. W. H. Freeman and Company New York, NY. 39, 1005-1041; 13, 315-330; 17, 397-426 (1988)
2. Mitchell, P. Coupling of phosphorylation to electron and hydrogen transfer by a chemi-osmotic type of mechanism. *Nature* 191, 144-148 (1961)
3. Okamoto, H., N. Sone, H. Hirota, M. Yoshida, and Y. Kagawa: Purified proton conductor in proton translocating adenosine triphosphatase of a thermophilic bacterium. *J Biol Chem* 252, 6125-6131 (1977)
4. Peschek, G.A.: Structure and function of respiratory membranes in cyanobacteria (blue-green algae) in subcellular biochemistry. Eds. D. Roodyn Plenum Press New York, NY. 85-191.

5. Luecke H., B. Schobert, H. T. Richter, J. P. Cartailler, and J. K. Lanyi: Structure of bacteriorhodopsin at 1.55 Å resolution. *Proc Natl Acad Sci USA* 291, 899-911 (1999)
6. Baciou, L., and H. Michel.: Interruption of the Water Chain in the Reaction Center from *rb. Sphaeroides* Reduces the Rate of Proton Uptake and of the Second Electron Transfer to Q_B . *Biochem* 34, 7967-7972 (1995)
7. Bartl, F., G. Deckers-Hebestreit, K. Altendorf, and G. Zundel: The F_0 complex of the ATP synthase of *Escherichia coli* contains a proton pathway with large proton polarizability caused by collective proton fluctuation. *Biophys J* 68, 104-110 (1995)
8. Cuma, M., U.W. Schmitt, and G.A. Voth: A multi-state empirical valence bond model for weak acid dissociation in aqueous solution. *J Phys Chem A* 105, 2814-2823 (2001)
9. Schmitt, U.W., and G.A. Voth: Multi-state empirical valence bond model for proton transport in water. *J Phys Chem B* 102, 5547-5551 (1998)
10. Schmitt, U.W., and G.A. Voth: The computer simulation of proton transport in water. *J Chem Phys* 111, 9361-9381 (1999a)
11. Schmitt, U.W., and G.A. Voth: Quantum properties of the excess proton in liquid water. *Isr J Chem* 39, 483-492 (1999b)
12. Schmitt, U.W., and G.A. Voth: The isotope substitution effect on the hydrated proton. *Chem. Phys. Lett.* 329, 36-41 (2000.)
13. Day, T.J.F., U.W. Schmitt, and G.A. Voth.: The mechanism of hydrated proton transport in water. *J Am Chem Soc* 122, 12027-12028 (2000)
14. Day, T.J.F., A.V. Soudakov, M. Cuma, U.W. Schmitt, and G.A. Voth: A second generation multistate empirical valence bond model for proton transport in aqueous systems. *J Chem Phys* 117, 5839-5849 (2002)
15. Brewer, M.L., U.W. Schmitt, and G.A. Voth: The formation and dynamics of proton wires in channel environments. *Biophys J* 80, 1691-1702 (2001)
16. Smondyrev, A.M. and G.A. Voth: Molecular dynamics simulation of proton transport near the surface of a phospholipid membrane. *Biophys J* 82, 1460-1468 (2002b)
17. Smondyrev, A.M., and G.A. Voth.: Molecular dynamics simulation of proton transport through the influenza A virus M2 channel. *Biophys J* 83, 1987-1996 (2002a)
18. Wu, Y., and G.A. Voth: Computational studies of proton transport through the M2 channel. *FEBS Lett.* (in press) (2003a)
19. Kim J., U.W. Schmitt, J.A. Gruetzmacher, G.A. Voth, and F. Scherer: The vibrational spectrum of the hydrated proton: comparison of experiment, simulation, and the normal mode analysis. *J Chem Phys* 116, 737-746 (2002)
20. Warshel, A.: 2.4 Proton transfer R_{xa} 's and the EVB model: Chapter 2 Chemical reactions in the gas phase and simple solvent models. Computer Modeling of Chemical Reactions in Enzymes and Solutions. J. Wiley and Sons-Interscience, New York 2.4, 55-59; 2, 40-73 (1991)
21. Vuilleumier, R., and D. Borgis: Molecular dynamics of an excess proton in water using a non-additive valence bond force field. *J Mol Struct* 436-437, 555-565. (1997)
22. Vuilleumier, R., and D. Borgis.: An extended empirical valence bond model for describing proton transfer in

- $H^+(H_2O)_n$ cluster and liquid water. *Chem Phys Lett* 284, 71-77 (1998a)
23. Vuilleumier, R., and D. Borgis: Quantum dynamics of an excess proton in water using an extended empirical valence-bond hamiltonian. *J Phys Chem* 102, 4261-4264 (1998b)
24. Lobaugh, J., and G.A. Voth: The quantum dynamics of an excess proton in water. *J Chem Phys* 104, 2056-2069 (1996.)
25. Mo, Y., and J. Gao: An *Ab Initio* molecular orbital-valence bond (MOVB) method for simulating chemical reactions in solution. *J Phys Chem A* 104, 3012-3020, and references therein (2000)
26. Zahn, D., and J. Brickmann: Quantum-classical simulation of proton transport via a phospholipid bilayer. *Chem Phys* 3, 848-852 (2001)
27. Walbran, S., and A. A. Kornyshev: Proton transport in polarizable water. *J Chem Phys* 114, 10039-10048 (2001)
28. Lill, M.A. and V. Helms: Molecular dynamics simulation of proton transport with quantum mechanically derived proton hopping rates (Q-HOP MD). *J Chem Phys* 115 (17), 7993-8005 (2001)
29. Webb, S.P., T. Iordanov, and S. Hammes-Schiffer: Multiconfigurational nuclear-electronic orbital approach: incorporation of nuclear quantum effects in electronic structure calculations," *J Chem Phys* 117, 4106-4118 (2002.)
30. Kumar, S., D. Bouzida, R. H. Swendsen, P. A. Kollman, and J. M. Rosenberg: The weighted histogram analysis method for free-energy calculations on biomolecules. I. The method. *J Comput Chem* 13, 1011-1021 (1992)
31. Cao, J., and G.A. Voth: A new perspective on quantum time correlation functions. *J Chem Phys* 99, 10070-10073 (1993)
32. Cao, J., and G.A. Voth: The formulation of quantum statistical mechanics based on the Feynman path centroid density. II. Dynamical Properties. *J Chem Phys* 100, 5106-5117 (1994a)
33. Cao, J., and G.A. Voth: The formulation of quantum statistical mechanics based on the Feynman path centroid density. III. Phase space formalism and analysis of centroid molecular dynamics. *J Chem Phys* 101, 6157-6167 (1994b)
34. Tuckerman, M., K. Laasonen, M. Sprik, and M. Parrinello: Ab initio molecular dynamics simulation of the solvation and transport of H_3O^+ and OH^- ions in water *J Chem Phys* 103, 150-161 (1995.)
35. Marx, M., M. E. Tuckerman, J. Hutter, and M. Parrinello: The nature of the hydrated excess proton in water. *Nature* London, England 397, 601-604 (1999)
36. Pomès, R., and B. Roux: Theoretical study of H^+ translocation along a model proton wire. *J Phys Chem* 100, 2519-2527 (1996a)
37. Pomès, R., and B. Roux: Structure and dynamics of a proton wire: A Theoretical study of H^+ translocation along the single file water chain in the gramicidin A channel. *Biophys J* 71, 19-39 (1996b)
38. Pomès, R., and B. Roux: Free energy profiles for H^+ conduction along hydrogen-bonded chains of water molecules. *Biophys J* 75, 33-40 (1998)
39. Pomès, R., and B. Roux: Molecular mechanism of H^+ conduction in the single-file water chain of the gramicidin channel. *Biophys J* 82, 2304-2316 (2002)
40. Stillinger, F.H., and C.W. David: Polarization model for water and its ionic dissociation products. *J Chem Phys* 69(4), 1473-1484 (1978)
41. Hummer, G., J. C. Rasaiah, and J. P. Noworyta: Water conduction through the hydrophobic channel of a carbon nanotube. *Nature* London, England 414, 188-190 (2001)
42. Dellago, C., M. M. Naor, and G. Hummer: Proton transport through water-filled carbon nanotubes. *Phys Rev Lett* 90, 105902-105905 (2003)
43. Lear, J.D., Z.R. Wasserman, W.F. DeGrado: Synthetic amphiphilic peptide models for protein ion channels. *Science* 240, 1177-1181 (1988)
44. Lear, J.D., J.P. Schneider, P.K. Kienker, and W.F. Drago: Electrostatic effects on ion selection and rectification in designed ion channels. *J Am Chem Soc* 119, 3212-3217 (1997)
45. Kienker, P.K., W.F. DeGrado, J.D. Lear: A helical-dipole model describes the single-channel current rectification of an uncharged peptide ion channel. *Proc. Natl. Acad. Sci. U.S.A.* 91, 4859 (1994)
46. Åkerfeldt, K.S., J.D. Lear, Z.R. Wasserman, L.A. Chung, and W.F. DeGrado: Synthetic peptides as models for ion channel proteins. *Acc. Chem. Res* 26, 191-197 (1993)
47. Mitton, P., and M.S.P. Sansom: Molecular Dynamics Simulations of Ion Channels Formed by Bundles of Amphiphathic α -Helical Peptides. *Eur. Biophys. J* 25, 139-150 (1996)
48. Zhong, Q., P.B. Moore, D.M. Newns, M.L. Klein: Molecular dynamics study of the LS3 voltage-gated ion channel. *FEBS Letters* 427, 267-270 (1998a)
49. Zhong, Q., Q. Jiang, P.B. Moore, D.M. Newns, and M.L. Klein: Molecular dynamics simulation of a synthetic ion channel. *Biophys. J* 74, 3-10 (1998b)
50. Randa, H.S., L.R. Forrest, G.A. Voth, and M. S. P. Sansom: Molecular dynamics of synthetic leucine-serine ion channels in a phospholipid membrane. *Biophys. J* 77, 2400-2410 (1999)
51. Wu, Y., and G.A. Voth: A computer simulation study of the hydrated proton in a synthetic proton channel. *Biophys. J* (in press) (2003b)
52. Bukrinskaya, A.G., N.K. Vorkunova, G.V. Kornilayeva, R.A. Narmanbetova, and G.K. Vorkunova: Influenza virus uncoating in infected cells and effect of rimantadine. *J. Gen. Virol* 60, 49-59 (1982)
53. Martin, K., and A. Helenius: Transport of incoming influenza virus nucleocapsids into the nucleus. *J. Virol* 65, 232-244 (1991)
54. Sugrue, R.J., and A.J. Hay: Structural Characteristics of the M2 Protein of Influenza A Viruses: Evidence that it forms a tetrameric channel. *Virology* 180, 617-624 (1991)
55. Wang, C., K. Takeuchi, L.H. Pinto, and R.A. Lamb: Ion channel activity of influenza A virus M2 protein: Characterization of the Amantadine Block. *J. Virol* 67, 5585-5594 (1993)
56. Wang, C., K. Takeuchi, L.H. Pinto, and R.A. Lamb: Ion channel activity of influenza A virus M2 protein: Characterization of the Amantadine Block. *J. Virol* 67, 585-5594 (1993)

Computer Simulation of Proton Transport

57. Ciampor, F., C.A. Thompson, S. Grambas, and A.J. Hay: Regulation of pH by the M2 protein of influenza A viruses. *Virus Res* 22, 247-258 (1992)
58. Grambas, S., and A.J. Hay: Maturation of influenza A virus hemagglutinin--estimates of the pH encountered during transport and its regulation by the M2 protein. *Virology* 190, 11-18 (1992)
59. Grambas, S., M.S. Bennett, and A.J. Hay: Influence of amantadine resistance mutations on the pH regulatory function of the M2 protein of influenza A viruses. *Virology* 191, 541-549 (1992)
60. Takeuchi, K., and R.A. Lamb: Influenza virus M2 protein ion channel activity stabilizes the native form of fowl plague virus hemagglutinin during intracellular transport. *J. Virol* 68, 911-919 (1994)
61. Sugrue, R.J., G. Bahadur, M.C. Zambon, M. Hall-Smith, A.R. Douglas, and A.J. Hay: Specific structural alteration of the influenza haemagglutinin by amantadine. *EMBO J.* 9, 3469-3476 (1990)
62. Holsinger, L.J., D. Nichani, L.H. Pinto, and R.A. Lamb: Influenza A virus M2 ion channel protein: A structure-function analysis. *J. Virol* 68, 1551-1563 (1994)
63. Pinto, L.H., G.R. Dieckmann, C.S. Gandhi, C.G. Papworth, J. Braman, M.A. Shaughnessy, J.D. Lear, R.A. Lamb, and W.F. DeGrado: A functionally defined model for the M2 proton channel of influenza A virus suggests a mechanism for its ion selectivity. *Proc. Natl. Acad. Sci. U. S. A.* 94, 11301-11306 (1997)
64. Bauer, C.M., L.H. Pinto, T.A. Cross, R.A. Lamb: The influenza virus M2 ion channel protein: probing the structure of the transmembrane domain in intact cells using engineered disulfide cross-linking. *Virology* 254 (1), 196-209 (1999)
65. Holsinger, L.J., and R.A. Lamb: Influenza virus M2 integral membrane protein is a homotetramer stabilized by formation of disulfide bonds. *Virology* 183, 32-43 (1991)
66. Kochendoerfer, G.G., D. Salom, J.D. Lear, R. Wilk-Orescan, S.B. Kent, and W.F. DeGrado: Total chemical synthesis of the integral membrane protein influenza A virus M2: Role of its C-terminal domain in tetramer assembly. *Biochemistry* 38, 11905-11913 (1999)
67. Sakaguchi, T., Q. Tu, L.H. Pinto, and R.A. Lamb: The active oligomeric state of the minimalistic influenza virus M2 ion channel is a tetramer. *Proc. Natl. Acad. Sci. U. S. A.* 94, 5000-5005 (1997)
68. Salom, D., B.R. Hill, J.D. Lear, and W.F. DeGrado: pH-dependent tetramerization and amantadine binding of the transmembrane helix of M2 from the influenza A virus. *Biochemistry* 39, 14160-14170 (2000)
69. Tian, C., K. Tobler, R.A. Lamb, L.H. Pinto, and T.A. Cross: Expression and initial structural insights from solid-state NMR of the M2 proton channel from influenza A virus. *Biochemistry* 41, 11294-11300 (2002)
70. Duff, K.C., and R.H. Ashley: The transmembrane domain of influenza A M2 protein forms amantadine-sensitive proton channels in planar lipid bilayers. *Virology* 190, 485-489 (1992)
71. Kovacs, F.A., and T.A. Cross: Transmembrane four-helix bundle of influenza A M2 protein channel: Structural implications from helix tilt and orientation. *Biophys. J.* 73, 2511-2517 (1997)
72. Kovacs, F.A., J.K. Denny, Z. Song, J.R. Quine, and T.A. Cross: Helix tilt of the M2 transmembrane peptide from influenza A virus: An intrinsic property. *J. Mol. Biol.* 295, 117-125 (2000)
73. Kukol, A., P.D. Adams, L.M. Rice, A.T. Brunger, and T.I. Arkin: Experimentally based orientational refinement of membrane protein mModels: A structure for the influenza A M2 H⁺ channel. *J. Mol. Biol.* 286, 951-962 (1999)
74. Song, Z., F.A. Kovacs, J. Wang, J.K. Denny, S.C. Shekar, J.R. Quine, and T.A. Cross: Transmembrane domain of M2 protein from influenza A virus studied by solid-state ¹⁵N polarization inversion spin exchange at magic angle NMR. *Biophys. J.* 79, 767-775 (2000)
75. Wang, J., S. Kim, F. Kovacs, and T.A. Cross: Structure of the transmembrane region of the M2 protein H⁺ channel. *Protein Sci* 10, 2241-2250 (2001)
76. Chizhmakov, I.V., D.C. Ogden, F.M. Geraghty, A. Hayhurst, A. Skinner, T. Betakova, and A.J. Hay: Differences in conductance of M2 proton channels of two influenza viruses at low and high pH. *J. Physiol* 546, 427-438 (2003)
77. Mould, J.A., J.E. Drury, S.M. Frings, U.B. Kaupp, A. Pekosz, R.A. Lamb, and L.H. Pinto: Permeation and activation of the M2 ion channel of influenza A virus. *J. Biol. Chem.* 275, 31038-31050 (2000)
78. Wang, C., R.A. Lamb, and L.H. Pinto: Activation of the M2 ion channel of influenza virus: A role for the transmembrane domain histidine residue. *Biophys. J.* 69, 1363-1371 (1995)
79. Gandhi, C.S., K. Shuck, J.D. Lear, G.R. Dieckmann, W.F. DeGrado, R.A. Lamb, and L.H. Pinto: Cu(II) Inhibition of the proton translocation machinery of the influenza A virus M2 protein. *J. Biol. Chem.* 274, 5474-5482 (1999)
80. Pinto, L.H., L.J. Holsinger, and R.A. Lamb: Influenza virus M2 protein has ion channel activity. *Cell* 69, 517-528 (1992)
81. Nishimura, K., S. Kim, L. Zhang, and T.A. Cross: The closed state of a H⁺ channel helical bundle combining precise orientational and distance restraints from solid state NMR. *Biochemistry* 41, 13170-13177 (2002)
82. Okada, A., T. Miura, and H. Takeuchi: Protonation of histidine and histidine-tryptophan interaction in the activation of the M2 ion channel from influenza a virus. *Biochemistry* 40, 6053-6060 (2001)
83. Tang, Y., F. Zaitseva, R.A. Lamb, and L.H. Pinto: The gate of the influenza virus M2 proton channel is formed by a single tryptophan residue. *J. Biol. Chem.* 277, 39880-39886 (2002)
84. Shuck, K., R.A. Lamb, and L.H. Pinto: Analysis of the pore structure of the influenza A virus M2 ion channel by the substituted-cysteine accessibility method. *J. Virol* 74, 7755-7761 (2000)
85. Sansom, M.S., I.D. Kerr, G.R. Smith, and H.S. Son: The Influenza A Virus M2 Channel: A molecular modeling and simulation study. *Virology* 233, 163-173 (1997)
86. Kaminski, G., R. A. Friesner, J. Tirado-Rives and W. L. Jorgensen: Evaluation and reparametrization of the OPLS-AA force field for proteins via comparison with accurate quantum chemical calculations on peptides. *J. Phys. Chem. B* 105, 6474-6487 (2001)
87. Lovell, S.C., J.M. Word, J.S. Richardson, and D.C. Richardson: The Penultimate Rotamer Library. *Proteins* 40, 389-408 (2000)

Computer Simulation of Proton Transport

88. Tajkhorshid, E., P. Nollert, M.O. Jensen, L.J. Miercke, J. O'Connell, R.M. Stroud, and K. Schulten. Control of the selectivity of the aquaporin water channel family by global orientational tuning. *Science* 296, 525-530 (2002)

89. Ciampor, F., P.M. Bayley, M.V. Nermut, E.M.A. Hirst, R.J. Sugrue, A.J. Hay: Evidence that the amantadine induced, M2 mediated conversion of influenza-A virus haemagglutinin to the low pH conformation occurs in an acidic trans-golgi compartment. *Virology* 188, 14-24 (1992)

Key Words: Proton, transport, Channels, molecular dynamics simulation, Computer, Review

Send correspondence to: Professor Gregory A. Voth, Department of Chemistry, University of Utah, 315 S. 1400 E., RM. 2020, Salt Lake City, UT. 84112-0850, Tel: 801-581-7272, Fax: 801-581-4353, E-mail: voth@chem.utah.edu